

Chapter 3

Fabrication

The total structure of MO pick-up contains four parts:

1. A sub-micro aperture underneath the SIL

The sub-micro aperture is used to limit the final spot size from 300nm to 600nm for NFR.

2. A microlens (SIL)

When the laser beam passes through the optical fiber and focused by SIL. The wavelength of light source will be reduced n times. So the spot size could be shrunk by SIL component.

3. A planar microcoil and the contact pad

The microcoil supplies a magnetic field (about 200~300Oe) to magnetize the heated spot on media surface. By Kerr Effect, the data can be written and read. The current density is inputted into the microcoil by the contact pad.

4. A support and bonding interface

The SU-8 is chosen as the material of support structure that is used to fix the total structure of MO pick-up head. The top surface of support is taken as bonding interface. This bonding interface will adhere to another element that included the optical fiber with a fiberlens in front-end, a 45°reflective lens, and a V-groove. The total MO pick-up head structure is shown as Fig.3-1.

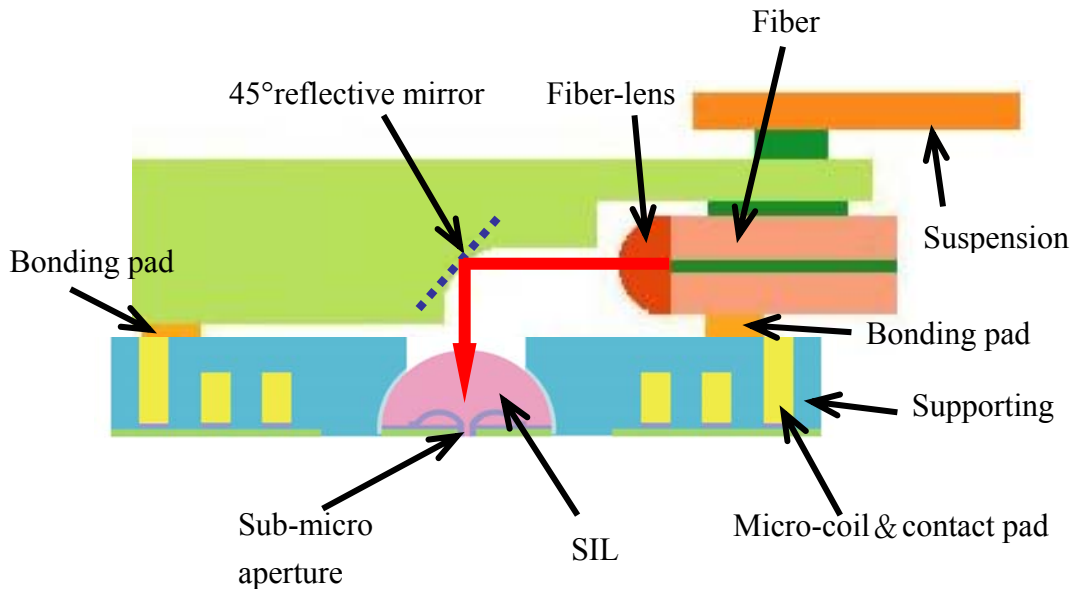
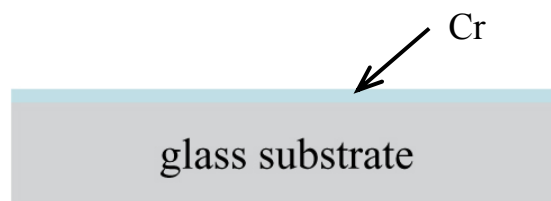


Fig.3-1 The total MO pick-up head structure

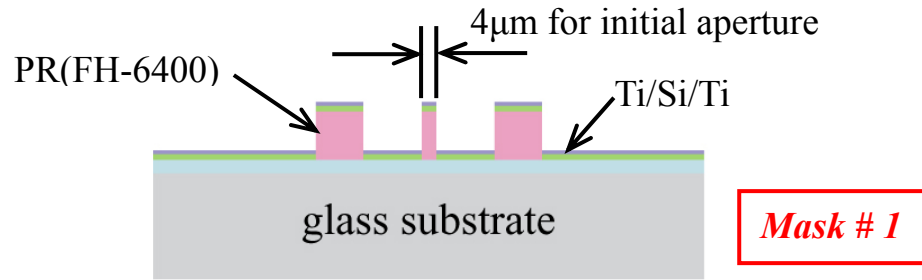


3.1 General Fabrication Flow-Chart

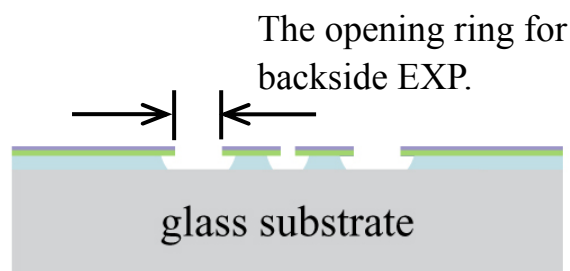
In this research, the MO pick-up head is made by surface micromachining and electroplating technology with seven masks and two backside exposure steps. Furthermore, the self-alignment technique is adopted to align precisely between the sub-micro aperture and the SIL. The general fabrication flowchart of MO pick-up is shown in Fig.3-2.



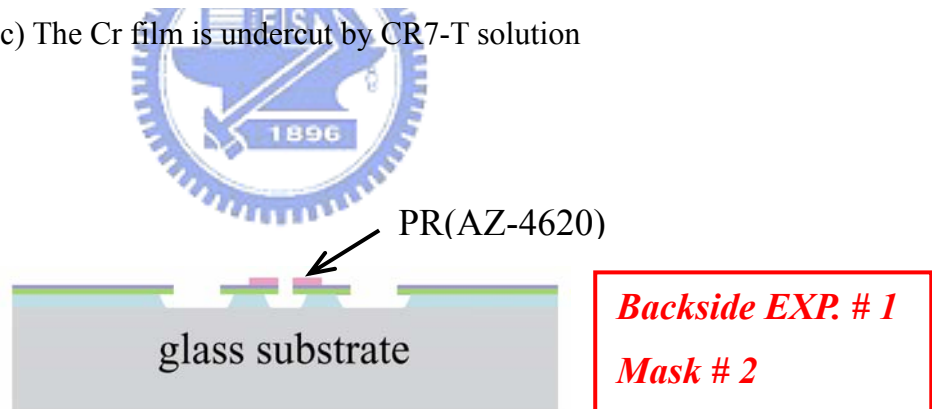
(a) The Cr film is deposited as the sacrificial layer



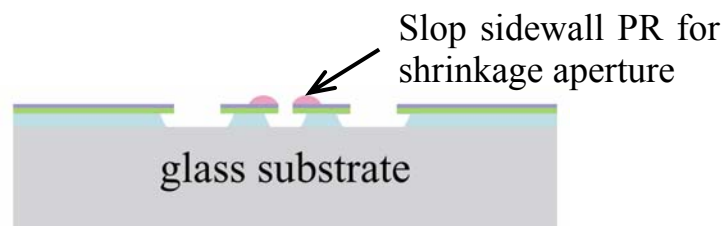
(b) The initial aperture is made into the Ti/Si/Ti pedestal layer by lift-off



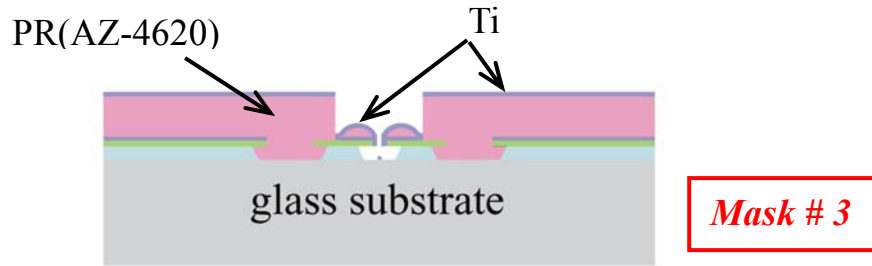
(c) The Cr film is undercut by CR7-T solution



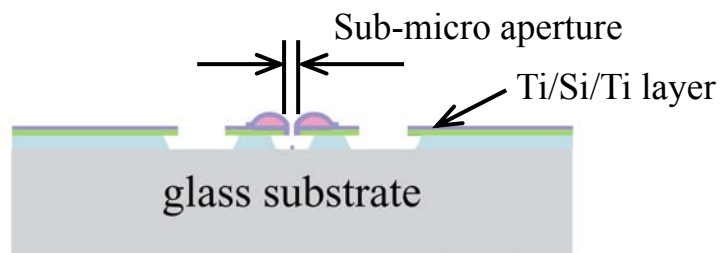
(d) The PR is patterned by Backside EXP. #1 and Mask #2



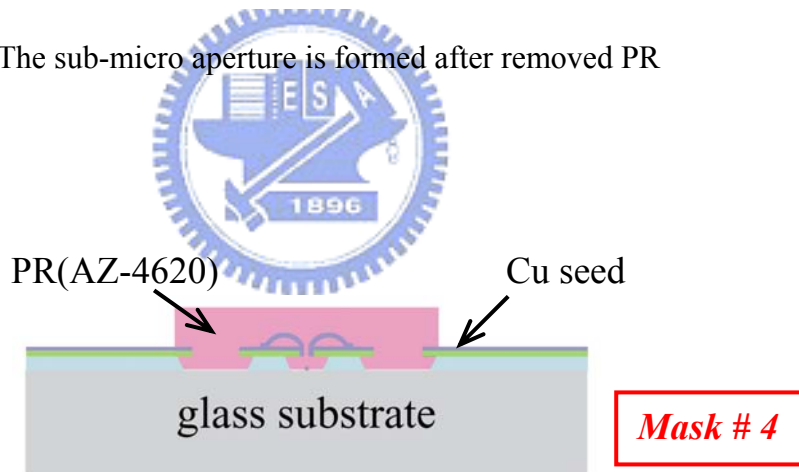
(e) The slop sidewall PR pattern is made by thermal reflowing



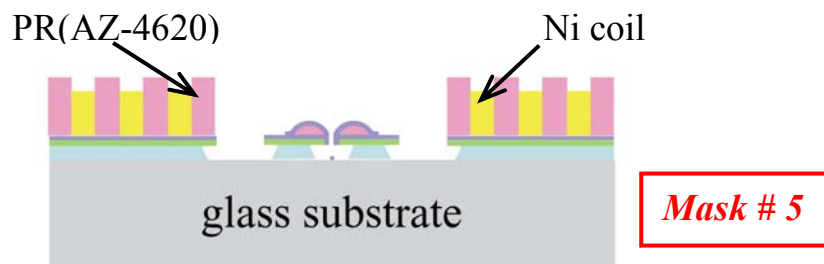
(f) The Ti metal is deposited by sputtering for shrinkage aperture



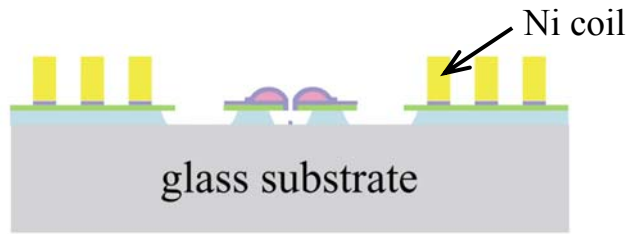
(g) The sub-micro aperture is formed after removed PR



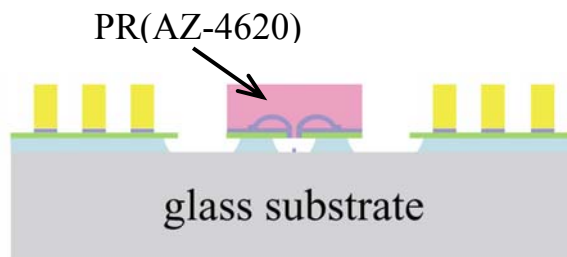
(h) The Cu seed is made by lift-off for electroplating coil



(i) Ni coil is fabricated by electroplating process

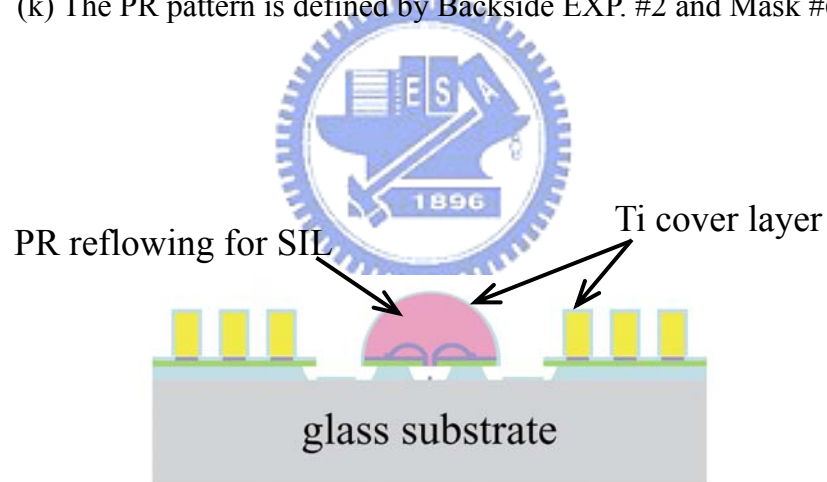


(j) Removing the PR coil mold

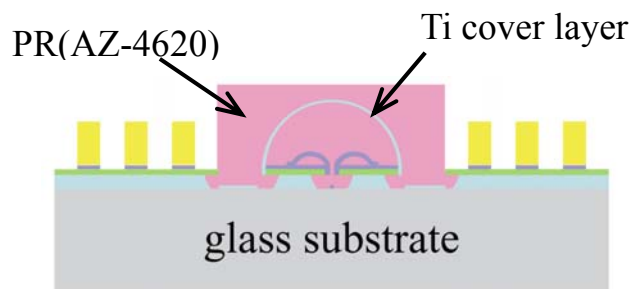


Backside EXP. # 2
Mask # 6

(k) The PR pattern is defined by Backside EXP. #2 and Mask #6

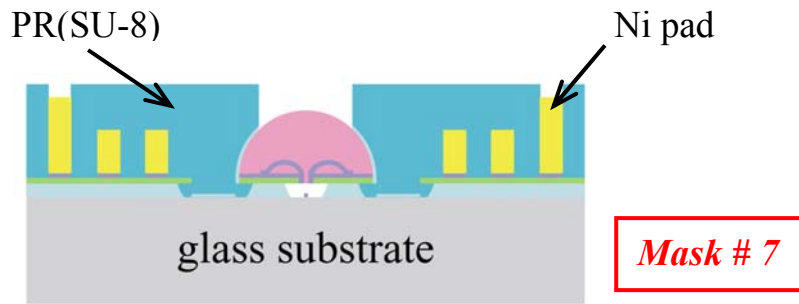


(l) The SIL is formed after reflowing, and Ti metal is deposited as cover layer

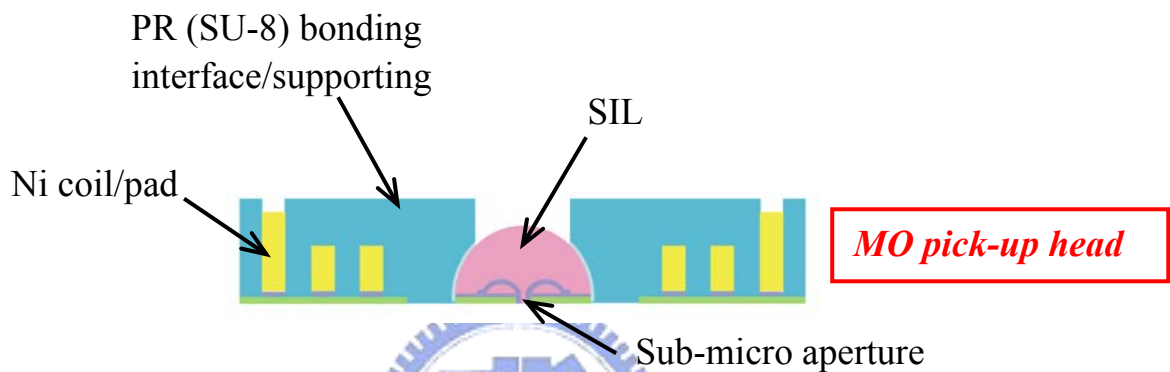


Mask # 4

(m) The Ti cover layer is etched by BOE



(n) PR (SU-8) is taken as supporting, and Ni pad is made by electroplating



(o) Etching Cr sacrificial layer by CR7-T for releasing

Fig.3-2 The general fabrication flowchart of MO pick-up

A Cr film $2\mu\text{m}$ is deposited on glass substrate by physical sputtering as the sacrificial layer (Fig.3-2(a)). The positive photoresist FH-6400 is spin-coated and patterned with mask #1. The initial aperture $4\mu\text{m}$ is made into the Ti/Si/Ti layer by lift-off process. This Ti/Si/Ti layer is deposited by physical sputtering (Fig.3-2(b)). Here, the Ti layer is taken as adhesion and cover layer to reduce the pin-hole effect in Cr film undercutting step efficiently. The α -Si is taken as the pedestal layer. The total structure of MO pick-up head will be fabricated above this α -Si pedestal layer. However, the thickness of Ti/Si/Ti layer must be less than 250nm for the aperture design in chapter 2. After lift-off process and Cr film undercutting, the initial aperture can be obtained. Furthermore, the opening ring is formed simultaneously. The UV

light can pass through this opening ring to fabricate the SIL in backside exposure step. By using self-alignment technique, the aperture and the SIL will be aligned precisely (Fig.3-2(c)). The detail self-alignment process will be described in next section.

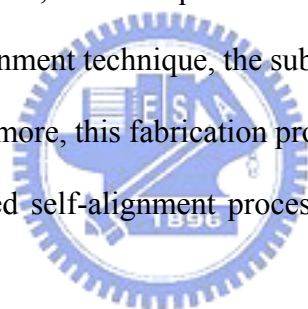
In order to shrink initial aperture size efficiently, a slope sidewall must be needed in initial aperture boundary. The positive photoresist AZ-4620 is spin-coated and defined with backside EXP. #1 and mask #2. Then, the PR ring is formed (Fig.3-2(d)). After thermal reflowing, the slope sidewall is created in initial aperture boundary (Fig.3-2(e)). The photoresist AZ-4620 is patterned by mask #3 for shrinkage aperture step. Then, the Ti metal is deposited by physical sputtering to shrink the initial aperture (Fig.3-2(f)). After removed photoresist, the final aperture that has a sub-micro scale is accomplished. This sub-micro aperture will limit the spot size from 300nm to 600nm for near-field recording (Fig.3-2(g)).

For electroplating Ni coil, the Cu seed layer is made by lift-off process. In this step, the photoresist AZ-4620 is defined by mask #4 (Fig.3-2(h)). Then, the thick film process and electroplating technique (UV LIGA technique) are adopted to fabricate the planar Ni coil. The positive photoresist AZ-4620 is spin-coated and patterned with mask #5 as the electroplating mold. The Cu seed layer is utilized to electroplate the Ni coil (Fig.3-2(i)). After removed the photoresist coil mold and Cu seed layer, the planar coil can be achieved (Fig.3-2(j)).

In order to fabricate the SIL easily, the positive photoresist AZ-4620 is chosen as the material of the SIL. The columnar photoresist pattern (AZ-4620 20 μ m) is defined with backside EXP. #2 and mask #6 (Fig.3-2(k)). By thermal reflowing, the SIL microlens can be formed. Furthermore, the sub-micro aperture and SIL can be aligned precisely due to the self-alignment technique. After, the Ti cover layer is deposited by physical sputtering to protect the SIL from chemical etching in the supporting fabrication step (Fig.3-2(l)).

Following, the positive photoresist AZ-4260 is spin-coated and patterned with mask #4. Then, the partial Ti cover layer is etched by BOE (Fig.3-2(m)). After removed photoresist AZ-4620, the negative photoresist SU-8 is patterned by mask #7 as the material of supporting. The top surface of the support is taken as bonding interface to combine another optics parts for complete MO pick-up head. Then, the Ti cover layer on the SIL is etched by BOE. So the light source can pass through the SIL, and is focused again by the SIL. After, the electroplating technique is employed again to make Ni pad for interconnections (Fig.3-2(n)). Finally, the Cr sacrificial layer is released by CR7-T chemical solution. Hence the structure of MO pick-up head will be achieved (Fig.3-2(o)).

In this fabrication process, the complex bonding or assembling process is discarded. By using self-alignment technique, the sub-micro aperture and the SIL can be aligned precisely. Furthermore, this fabrication process is a batch process, and it is a stable process. The detailed self-alignment process will be described in the next section.

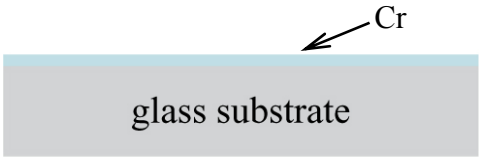
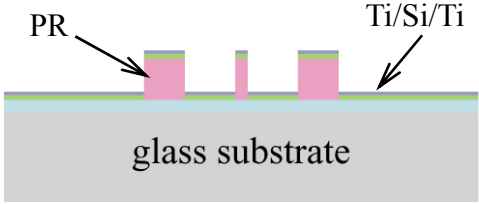
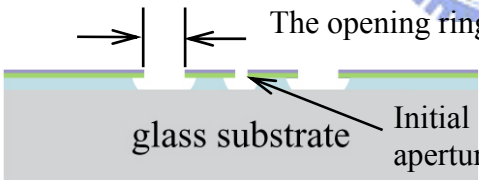
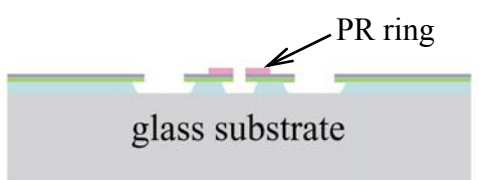
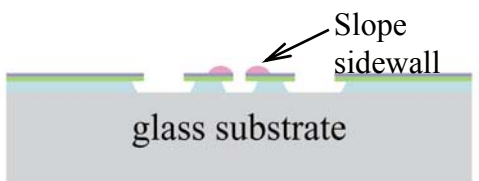


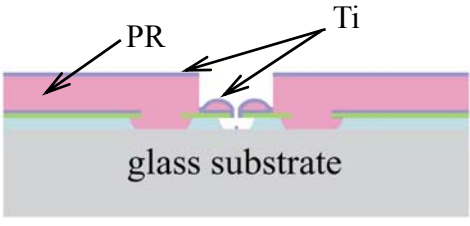
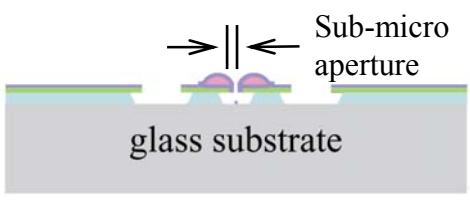
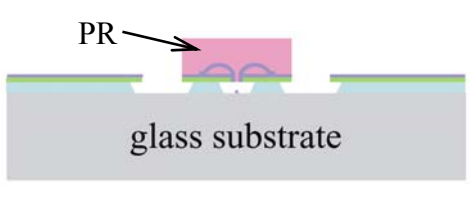
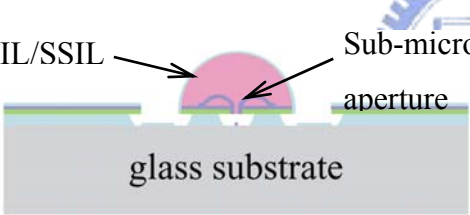
3.2 Fabrication in Self-Alignment Process

The glass substrate is chosen for self-alignment technique, which is based on the backside exposure. First, the initial aperture is made into the Ti/Si/Ti layer by lift-off process, and this Ti/Si/Ti layer is taken as the mask pattern for the backside exposure step. After undercut Cr sacrificial layer, the initial aperture and opening ring are formed simultaneously. The light source can pass through this opening ring to expose the photoresister for backside exposure step. By the backside exposure step, the columnar photoresist pattern can be created. Then, the thermal reflowing process is applied to fabricate the SIL. Owing to the pattern of initial aperture and opening ring

is a concentric circle structure, and fabricated in the same process step. Hence the SIL and aperture can be aligned together precisely by self-alignment technique. The self-alignment process is shown in Tab.3-1.

Tab.3-1 Fabrication in self-alignment process

<i>Process diagram</i>	<i>Process step</i>
<p>a.</p>  <p style="text-align: center;">glass substrate</p>	<p>1. Deposited Cr film 2μm by physical sputtering as the sacrificial layer</p>
<p>b.</p>  <p style="text-align: center;">glass substrate</p>	<p>2. Photoresist FH-6400 2μm is defined with mask #1 3. The Ti/Si/Ti layer is deposited by sputtering (the total thickness must be less than 250nm) 4. The initial aperture is made into this Ti/Si/Ti layer by lift-off process</p>
<p>c.</p>  <p style="text-align: center;">glass substrate</p>	<p>5. After lift-off process, the Cr sacrificial film is etched by CR7-T for undercutting (the opening ring and initial aperture size 4μm can be formed simultaneously)</p>
<p>d.</p>  <p style="text-align: center;">glass substrate</p>	<p>6. The photoresist AZ-4620 is patterned by backside EXP. #1 (Ti/Si/Ti pattern) and mask #2, then the PR pattern ring can be obtained</p>
<p>e.</p>  <p style="text-align: center;">glass substrate</p>	<p>7. After thermal reflowing, the slope sidewall is created in initial aperture boundary (this slope sidewall for shrinkage aperture)</p>

<p>f.</p>  <p>PR</p> <p>Ti</p> <p>glass substrate</p>	<p>8. Photoresist AZ-4620 is patterned with mask #3</p> <p>9. The Ti metal is deposited by physical sputtering to shrink the initial aperture</p>
<p>g.</p>  <p>Sub-micro aperture</p> <p>glass substrate</p>	<p>10. After removed photoresist, the sub-micro aperture is achieved (about 300~500nm for NRF)</p>
<p>h.</p>  <p>PR</p> <p>glass substrate</p>	<p>11. The columnar photoresist AZ-4620 pattern is defined with backside EXP. #2 (Ti/Si/Ti pattern) and mask #6</p>
<p>i.</p>  <p>SIL/SSIL</p> <p>Sub-micro aperture</p> <p>glass substrate</p>	<p>12. After thermal reflowing, the SIL microlens can be obtained, moreover, the SIL and the sub-micro aperture will be aligned precisely by self alignment process</p>

3.3 Process of Sub-micro Aperture Fabrication

The initial aperture is fabricated into the Ti/Si/Ti pedestal layer by lift-off process, and shrunk by physical sputtering until the diameter of aperture arrives in sub-micro scale (300~500nm). The design parameters of the sub-micro aperture are discussed in chapter 2. The fabrication flowcharts and process steps are shown in Tab.3-1(a)-(g).

The initial aperture $4\ \mu\text{m}$ and opening ring pattern are defined with mask #1 as shown in Fig.3-3(a). This opening ring has two functions, one is for fabricating SIL in backside exposure step and the other is for deciding diameter of SIL. After sputtering Ti/Si/Ti pedestal layer and lift-off process, the initial aperture $4\ \mu\text{m}$ and

opening ring will be achieved as shown in Fig3-3(b). Then, the undercutting process is adopted to etch the sacrificial layer unit the glass in initial aperture and opening ring is appeared, as shown in Fig.3-3(c).

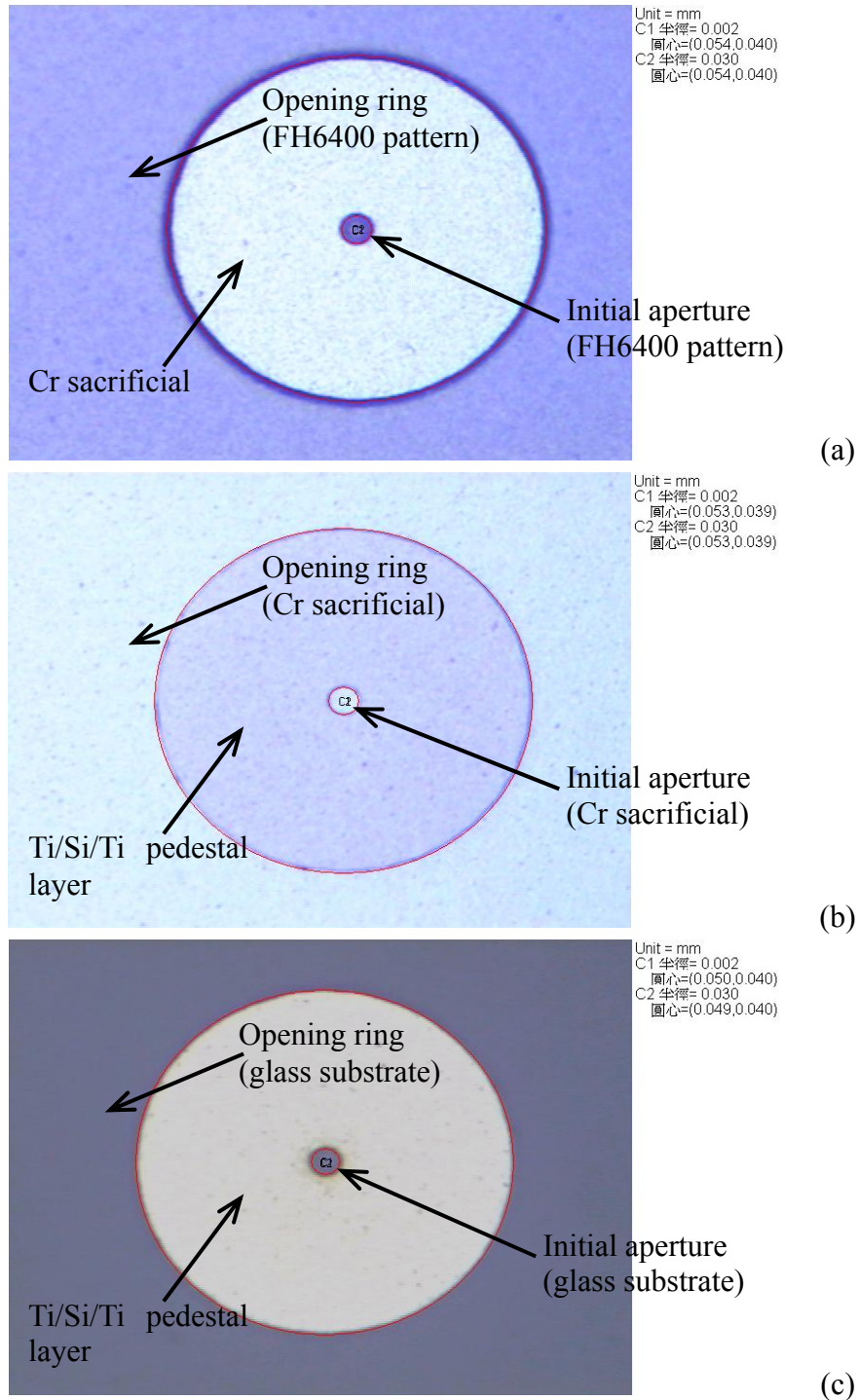


Fig.3-3 Initial aperture $4\mu\text{m}$ and opening ring pattern (a) Photoresister FH6400 pattern (b) After lift-off process (c) After undercutting process

Then, the sputtering technique is applied to shrink initial aperture. In order to shrink initial aperture size efficiently, a slop sidewall must be needed in initial aperture boundary. Owing to the slope sidewall in initial aperture boundary, the step coverage expected to be improved in physical sputtering process. The slop sidewall is made by thermal reflowing. The first, the PR ring pattern is defined with backside EXP. #1 and mask #2. By the self-alignment technique, the inner circle of PR ring and initial aperture boundary can be aligned together precisely, as shown in Fig.3-4. Then, the PR ring is heated at 150°C for 2 hours for thermal reflowing process. Hence a slope sidewall can be obtained in initial aperture boundary. The fabrication result of initial aperture with a slope sidewall in aperture boundary is shown in Fig.3-5(a), and a initial aperture of diameter 2.88 μm is shown in Fig.3-5(b).

After slope sidewall fabrication, the photoresister AZ-4620 8 μm is patterned with mask #3 to protect the opening ring from depositing metal in shrinkage initial aperture step. The fabrication results are shown in Fig.3-6(a) and Fig.3-6(b), respectively.

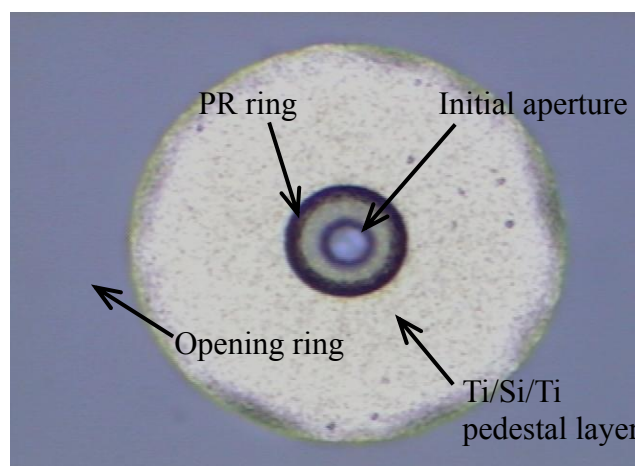


Fig.3-4 The photoresister ring pattern in initial aperture boundary before reflowing

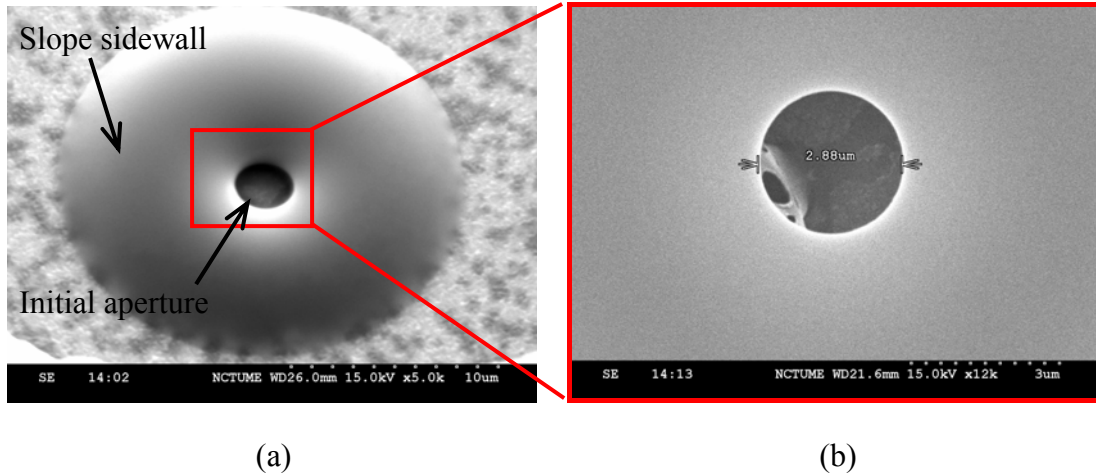


Fig.3-5 (a) A slope sidewall in initial aperture boundary after reflowing (b) The aperture with diameter of 2.88 μ m

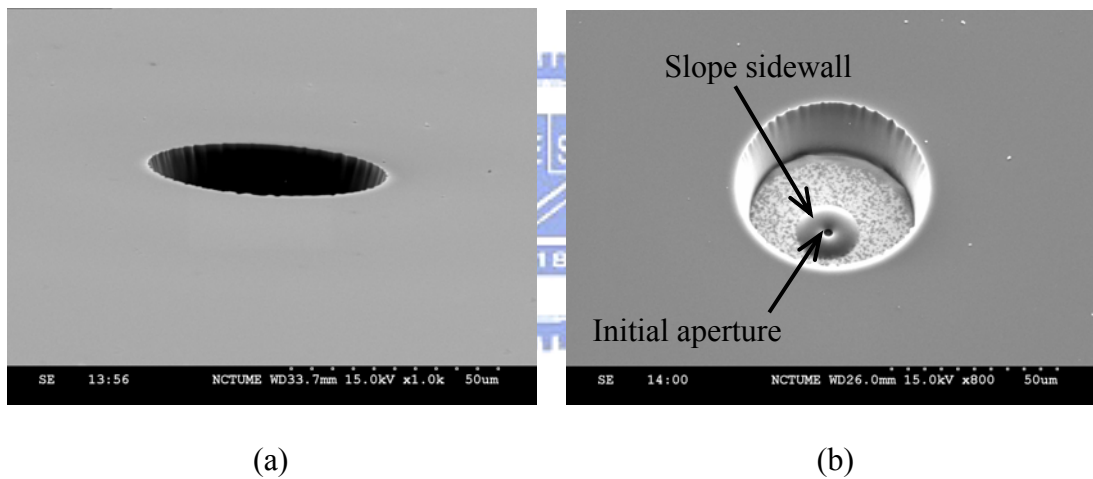


Fig.3-6 The photoresist AZ4620 pattern for shrinkage initial aperture (a) The lateral view (b) The top view

We adjust a lot of parameters of physical sputtering in shrinkage initial aperture step as shown in Tab.3-2. In Tab.3-2, the sputter equipment uses DC gun only, and all of the parameters of sputtering have failed in shrinkage initial aperture step. We found a reason that the step coverage was very poor in using DC gun only. Hence the initial aperture is not shrunk by DC gun sputtering. According to related information of physical sputtering, it is known that the step coverage can be improved

by increasing work pressure or arrival angle on substrate. For this reason, we employed double gun sputtering including DC and RF gun to increase arrival angle for improvement step coverage. Furthermore, the work pressure is increased to improve step coverage, too. The parameters of double gun sputtering is listed in Tab.3-3, and the fabrication results of initial aperture before and after shrinkage process are shown in Fig.3-7(a) and Fig.3-7(b), respectively. In double gun sputtering process, the initial aperture of diameter $4.55 \mu\text{m}$ uses the parameters of function one of Tab.3-3. to shrink aperture size. The aperture of diameter $4.05 \mu\text{m}$ can be obtained after double gun sputtering process. We found that the shrinkage efficiency was so bad. Hence the shrinkage aperture process by using double gun sputtering is still failing. We don't know the reason which the shrinkage aperture by physical sputtering is failed. But we don't have give up. The thermal coater process is adopted to shrink initial aperture again, but the shrinkage efficiency is still bad. The parameters of photolithography are listed in Tab.3-4, and sputtering equipment is shown in Fig.3-8.

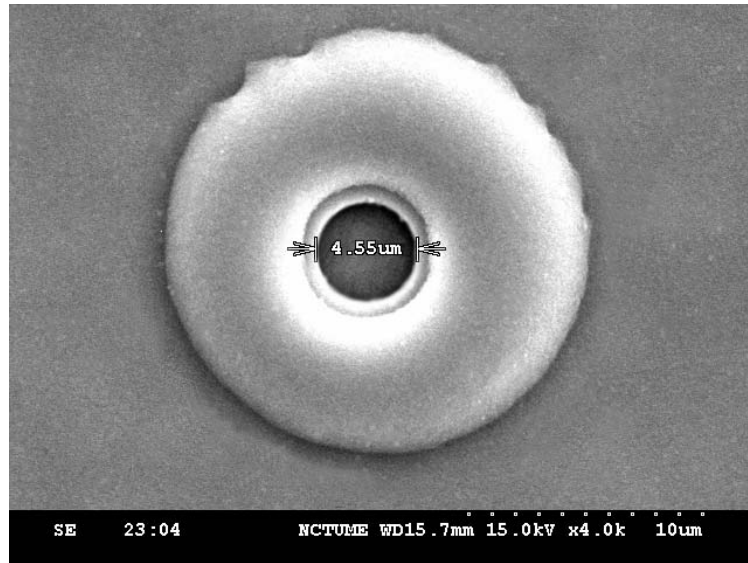
In this research, the shrinkage initial aperture by physical sputtering or thermal coater is failing. But we think that the physical sputtering or thermal coater techniques are a feasible process for shrinkage aperture. Furthermore, we bring up two techniques including the electroplating process and electro-beam (E-beam) writer can also fabricate the sub-micro aperture.

Tab.3-2 The parameters of physical sputtering (DC gun only)

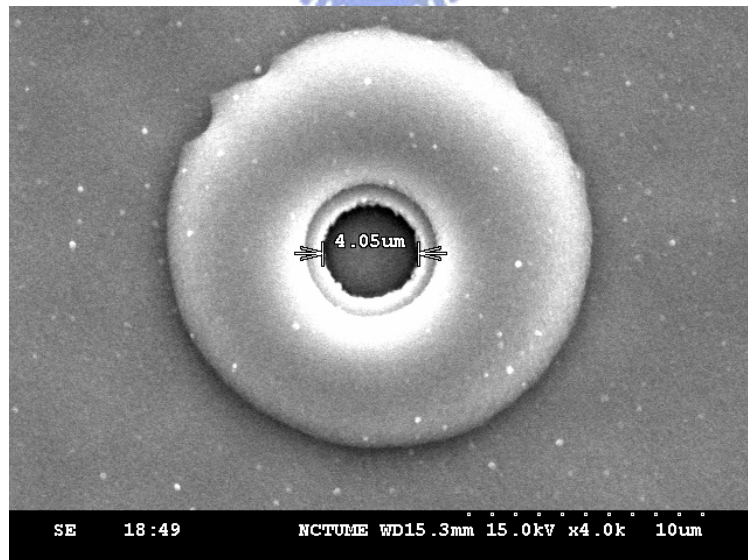
metal	Current (A)	Pressure (mTorr)	RPM.	Ar gas (sccm)	worktime	Temp range (°C)
Ni	0.5	4.5	50	20	2hr30min	23~32
Ni	0.5	4.5	10	20	3hr	23~36
Cr	0.2	4.5	50	20	1hr30min	24~29
Cr	0.2	100	50	20	1hr30min	22~31

Tab.3-3 The parameters of physical sputtering (DC and RF gun)

	gun	Metal	Watt (W)	Pressure (mTorr)	RPM.	Ar gas (sccm)	work time	Temp (°C)
1	DC	Ti	120	50	50	20	1hr	45~51
	RF	Ti	150	50	50	20	1hr	45~51
2	DC	Ti	130	4.5	50	20	2hr	43~56
	RF	Ti	150	4.5	50	20	2hr	43~56



(a)



(b)

Fig.3-7 The diameter of aperture (a) before shrinkage process with 4.55 μ m (b) after shrinkage process with 4.05 μ m

Tab.3-4 Parameters of photolithography

Item	Variable		
<i>Photo-resist</i>	FH-6400 [2 μ m] Lift-off process	AZ-P4620 [5 μ m] PR ring pattern	AZ-P4620 [8 μ m] Shrinkage aperture Cu seed lift-off
<i>First spin rpm time</i>	1000 rpm 5 sec	1500 rpm 10 sec	1000 rpm 10 sec
<i>Second spin rpm time</i>	1000 rpm 30 sec	3000 rpm 40 sec	2500 rpm 25 sec
<i>Soft-bake time</i>	90°C 90 sec	90°C 15 mins	90°C 20 mins
<i>Exposure</i>	2.3 sec	5 sec	12 sec
<i>Development</i>	30~35 sec [FHD-5]	100~110sec [FHD-5]	120~130sec [FHD-5]

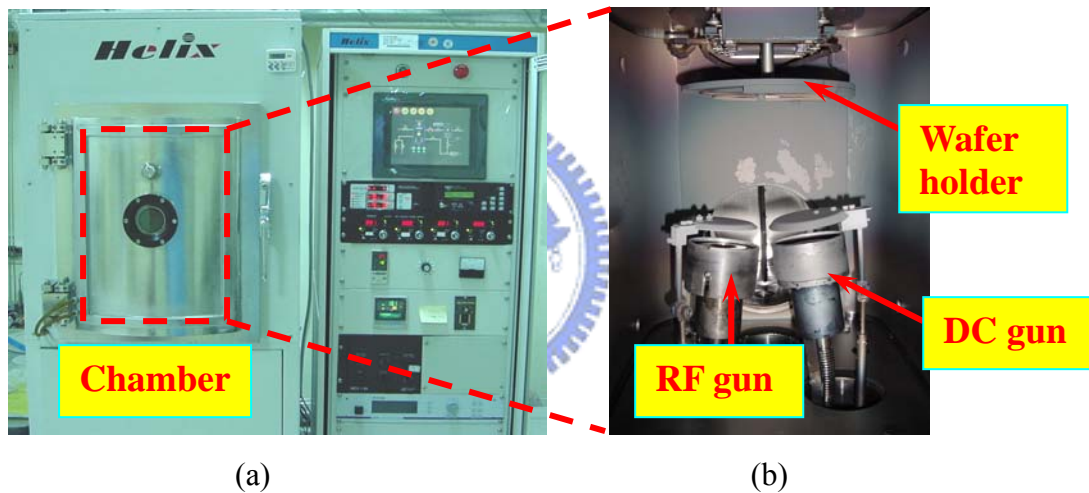


Fig.3-8 (a) The view of sputtering equipment (b) The gun of target and wafer holder

3.4 Process of SIL Fabrication

In this research, the photoresist AZ-4620 is chosen as the material of the SIL. By using the thermal reflowing process, the SIL component can be achieved easily. The basic theory of thermal reflowing and fabrication of the SIL will be described in the following.

3.4.1 Basic Theory of Thermal Reflowing

When the patterned photoresist is heated over its glass transition temperature (T_g) on the substrate. It begins to melt and the liquid-like photoresist tends to minimize its surface in order to reduce the surface energy. At the same time, the contact angle will change with the variation of surface energy until the stable state. The basic principle of the shape transformation before and after thermal reflowing process is shown in Fig.3-9.

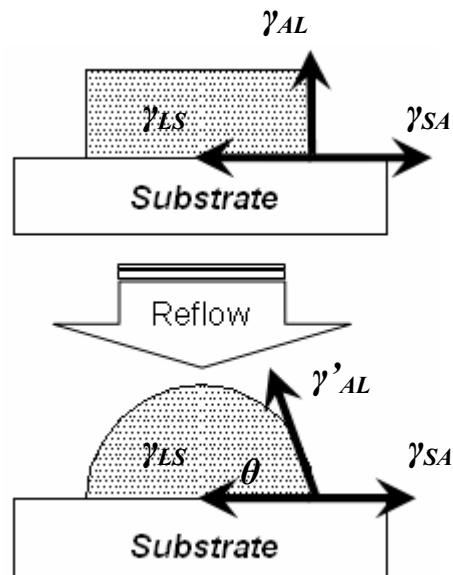


Fig.3-9 Illustration of profile change before and after thermal reflow process

According to the concept of static equilibrium, the function of equilibrium can be written as the following equations :

$$\gamma_{SA} = \gamma_{LS} \quad (\text{Before thermal reflow}) \quad (1)$$

$$\gamma_{SA} = \gamma_{LS} + \gamma'_{AL} \cos \theta \quad (\text{After thermal reflow}) \quad (2)$$

γ_{SA} : the surface energy of the solid-air

γ_{LS} : the interface energy of the liquid-solid

γ_{AL} : the surface tension of the air-liquid before thermal reflow

γ'_{AL} : the surface tension of the air-liquid after thermal reflow

θ : the equilibrium contact angle

γ_{AL} represents the high surface energy as pattern while γ'_{AL} shows the minimum surface energy after thermal reflowing process. Since the surface energy changes from γ_{AL} to γ'_{AL} , the contact angle θ alters in compliance with the rule of equilibrium equation (2). Therefore, a microlens can be fabricated with a smooth surface.

3.4.2 Fabrication of SIL

The SIL component is located above the sub-micro aperture. The design parameters of the SIL are discussed in chapter 2. The photoresist AZ-4620 will be chosen as the material of the SIL due to the easy reflowing characteristics. The fabrication flowcharts and process steps are shown in Tab.3-1(h)-(i). The fabrication results will compare with the designed parameters, and are discussed in the following.

The columnar photoresist AZ-4620 20 μ m pattern is defined with backside EXP.#2 and mask #6 for SIL fabricating. Here, the Ti/Si/Ti pedestal layer is taken as the mask for backside exposure. Owing to the pattern of aperture and opening ring is a concentric circle structure, and fabricated in the same process step. So the aperture and SIL will be aligned together precisely by self-alignment technique. The illustration of backside exposure mechanism is shown in Fig.3-10. The UV light can pass through the opening ring to expose the photoresist AZ-4620 in backside exposure step, and then the photoresist AZ-4620 is exposed with mask #6 continuously. After

development step, a columnar pattern of AZ-4620 is formed.

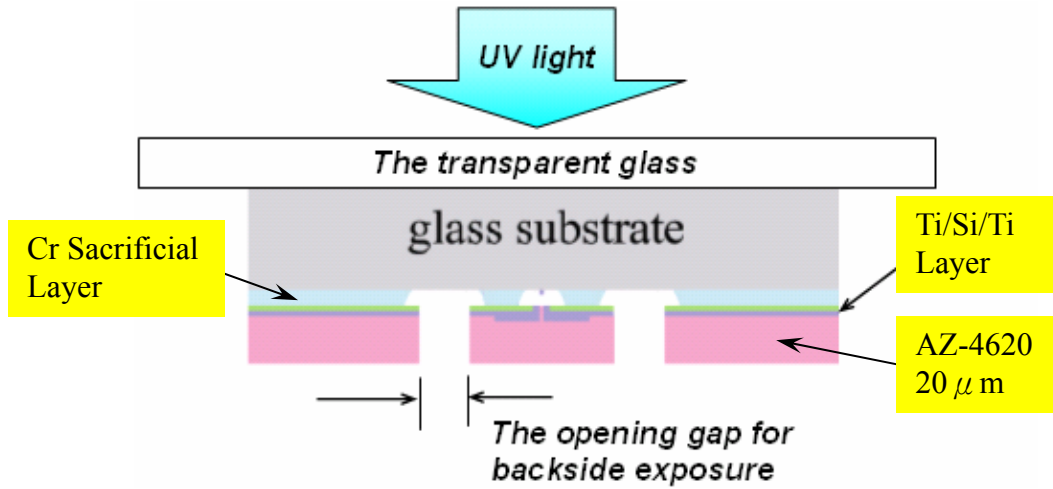


Fig.3-10 Backside exposure mechanism

In this research, the diameter of SIL is designed with $60 \mu\text{m}$ and $70 \mu\text{m}$, and the thickness of photoresister AZ-4620 is decided with $20 \mu\text{m}$, as shown in Tab.2-2. The fabrication result of columnar PR AZ-4620 thickness is measured by two-dimension surface profiler as shown in Fig.3-11, this result match with the designed parameters. The columnar pattern of AZ-4620 of diameter $58.57 \mu\text{m}$ and $68.26 \mu\text{m}$ are measured by Scanning Electron Microscope (SEM) system, and the fabrication results are shown in Fig.3-12(a) and Fig.3-12(b), respectively. We can find that a lost dimension in the diameter of columnar AZ-4620 pattern compared with the designed parameters of SIL diameter, this lost dimension occurred in backside exposure step. Because of the diffraction always exists in UV light exposure step, so a lost dimension in the diameter of columnar AZ-4620 pattern will produce in backside exposure step due to diffraction effect. The fabrication result of backside exposure and the diffraction phenomenon in backside exposure step are shown in Fig.3-13(a) and Fig.3-13(b), respectively.

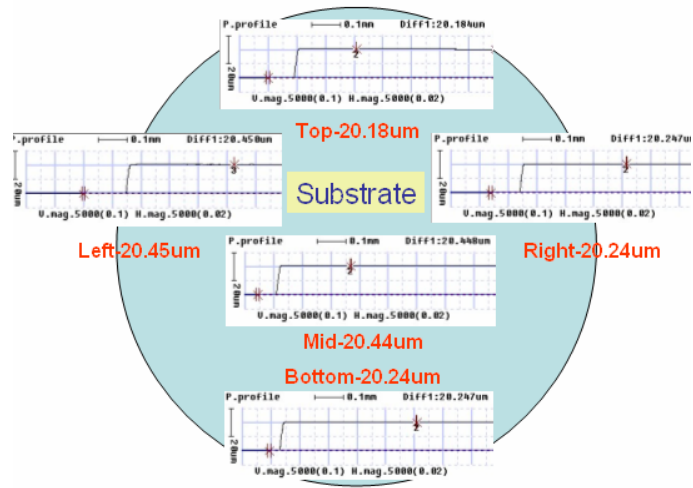
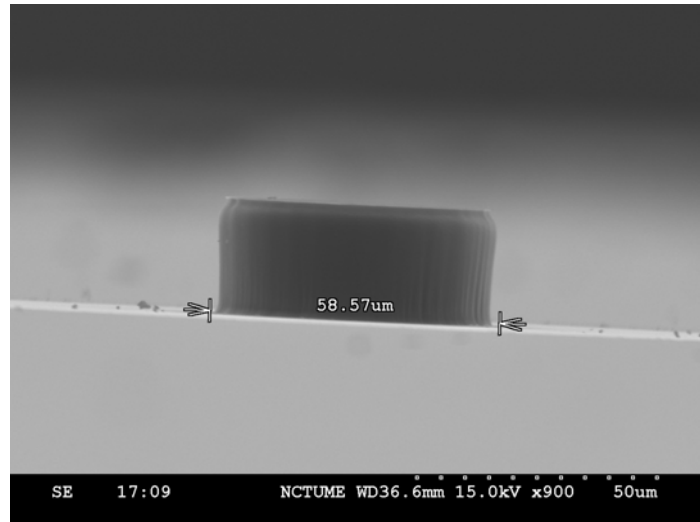
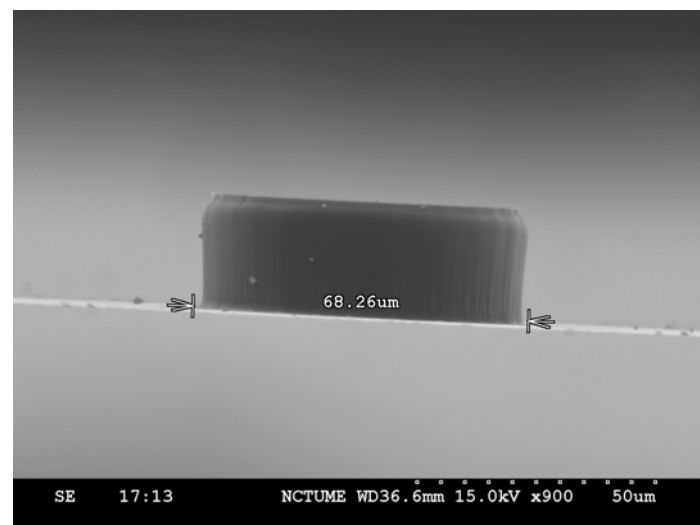


Fig.3-11 The fabrication result of PR AZ-4620 thickness

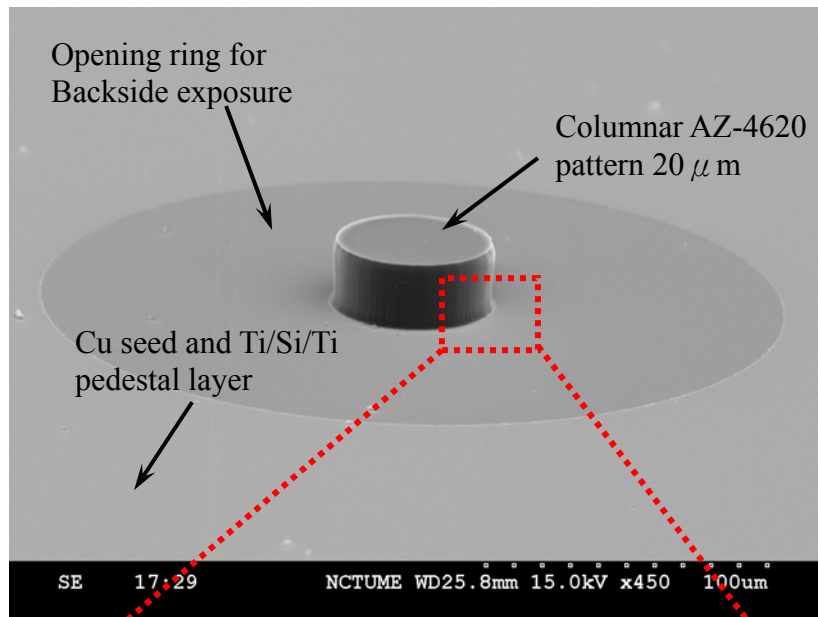


(a)

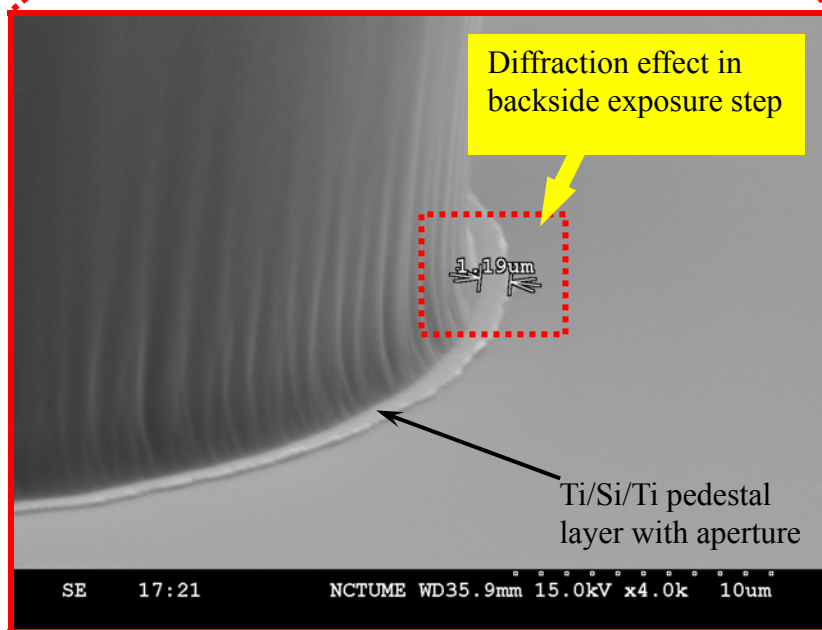


(b)

Fig.3-12 The diameter of columnar pattern AZ-4620 is (a) $58.57 \mu\text{m}$ (b) $68.26 \mu\text{m}$



(a)



(b)

Fig.3-13 (a) The result of backside exposure (b) the diffraction phenomenon in backside exposure step

After backside exposure step, the columnar pattern of AZ-4620 is heated at 150° C for 2.5 hours by the oven. By using thermal reflowing process, the SIL component can be achieved. The fabrication results of before and after thermal reflowing are

shown in Fig.3-14(a) and Fig.3-14(b), respectively. The surface profiles of SIL component are measured with 2-D and 3-D surface profiler. The 3-D profile measurement results of SIL component of diameter $60\ \mu\text{m}$ and $70\ \mu\text{m}$ are shown in Fig.3-15(a) and Fig.3-15(b). This 3-D profile will be transferred to 2-D curve pictures for measuring sag height of SIL component, as shown in Fig.3-16(a) and Fig.3-16(b). The maximum surface profile in 2-D curve pictures are captured, and measured again by 2-D surface profiler. Hence the real size of curvature and sag height of SIL component can be measured and obtained, and the measurement results are shown in Fig.3-17(a) and 3-17(b). The SIL of diameter $56.26\ \mu\text{m}$ and $66.92\ \mu\text{m}$ are measured and captured by SEM system as shown in Fig.3-18(a) and Fig.3-18(b). We measure and capture a lot of surface profile data of SIL by surface profiler and SEM system. The designed parameters and fabrication results of surface profile of SIL are listed in Tab.3-5. In Tab.3-5, the parameters of t , D , h , and r are the designed parameters as shown in Fig.2-10. The parameters of t' , D' , h' , and r' are the fabrication results. The Δh and Δr are the deviation between the designed parameters and fabrication results in sag size and radius size of SIL.

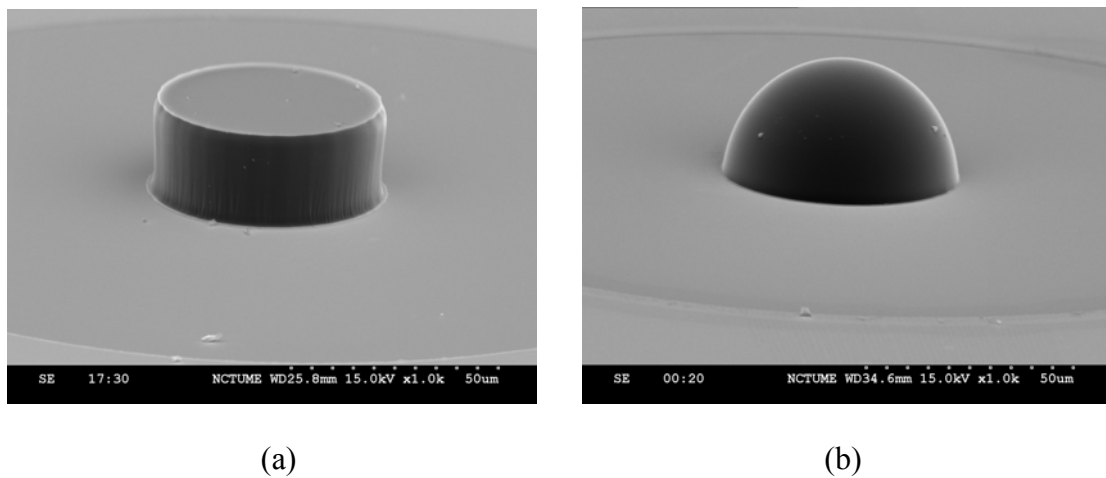


Fig.3-14 The fabrication results of SIL (a) before reflowing (b) after reflowing

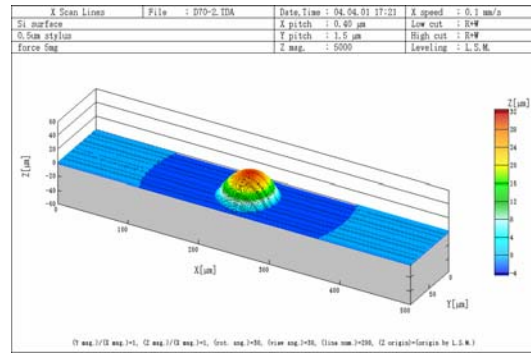
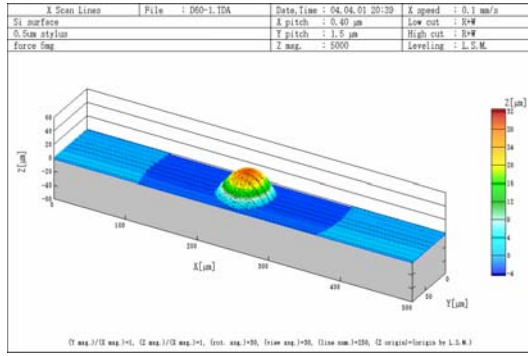


Fig.3-15 The 3-D profile measuring results of SIL of diameter (a) 60 μ m (b) 70 μ m

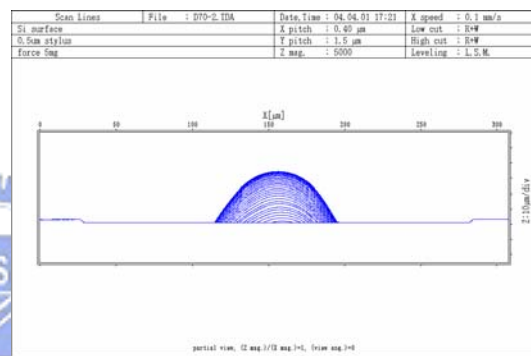
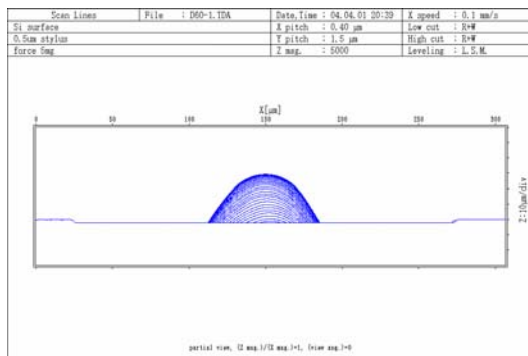


Fig.3-16 The 2-D curve measuring results of SIL of diameter (a) 60 μ m (b) 70 μ m

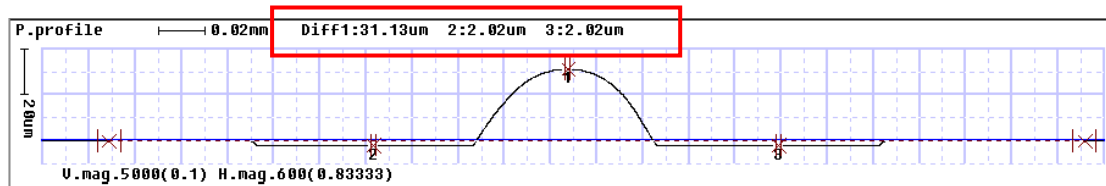
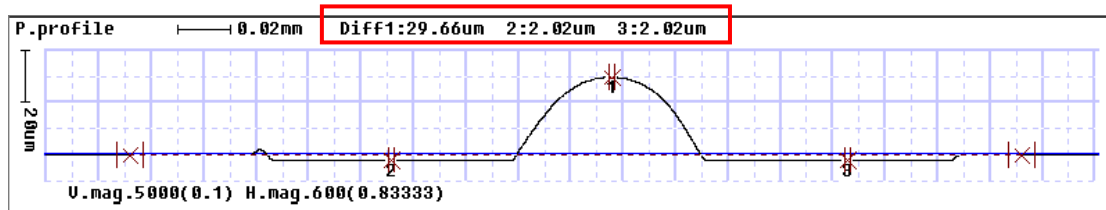
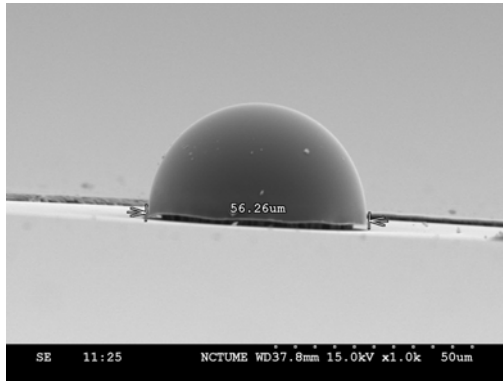
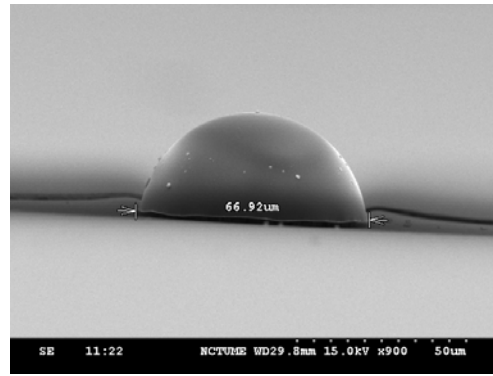


Fig.3-17 The real surface profile data of SIL of diameter (a) 60 μ m (b) 70 μ m



(a)



(b)

Fig.3-18 The SIL of diameter after reflowing with (a) 56.26 μ m (b) 66.92 μ m

Tab.3-5 The designed parameters and fabrication results of surface profile of SIL

SIL	<i>Designed parameters</i>				<i>Fabrication results</i>				<i>Deviation</i>	
	t (μ m)	D (μ m)	h (μ m)	r (μ m)	t' (μ m)	D' (μ m)	h' (μ m)	r' (μ m)	Δ h (%)	Δ r (%)
φ60	20	60	30.00	30.00	20.2	56.26	29.86	28.18	0.47	6.07
						57.07	29.63	28.56	1.23	4.82
						57.09	29.66	28.57	1.13	4.78
						57.22	29.74	28.63	0.87	4.56
φ70		70	31.50	35.19		66.73	31.28	33.43	0.69	4.99
						66.79	31.13	33.48	1.17	4.87
						66.78	30.92	33.49	1.83	4.83
						66.92	31.44	33.52	0.18	4.73

From above the table, we can find that the deviation in sag size of SIL was less than 2%. It is a good result in fabrication process, and the fabrication processes in this research are a stable process. But owing to the surface profile of SIL component is not a perfect hemisphere after thermal reflowing process. Because of the SIL is not a perfect hemisphere in fabrication result, so we will obtain a larger deviation in radius size of SIL. From Tab.3-5, we can find that the deviation in radius size of SIL is over 4.5%, this is a worse result. The parameters of photolithography are listed in Tab.3-6. The illustration of exposer equipment is shown in Fig.3-19.

Tab.3-6 Parameters of photolithography

Item	Variable
<i>Photo-resist</i>	AZ-P4620 [20 μ m] For SIL process / For electroplating mold
<i>First spin rpm</i> <i>time</i>	500 rpm 10 sec
<i>Second spin rpm</i> <i>time</i>	500 rpm 45 sec
<i>Soft-bake</i> <i>time</i>	90°C 20 mins
<i>Exposure</i>	25 sec
<i>Development</i>	4~5mins [FHD-5]

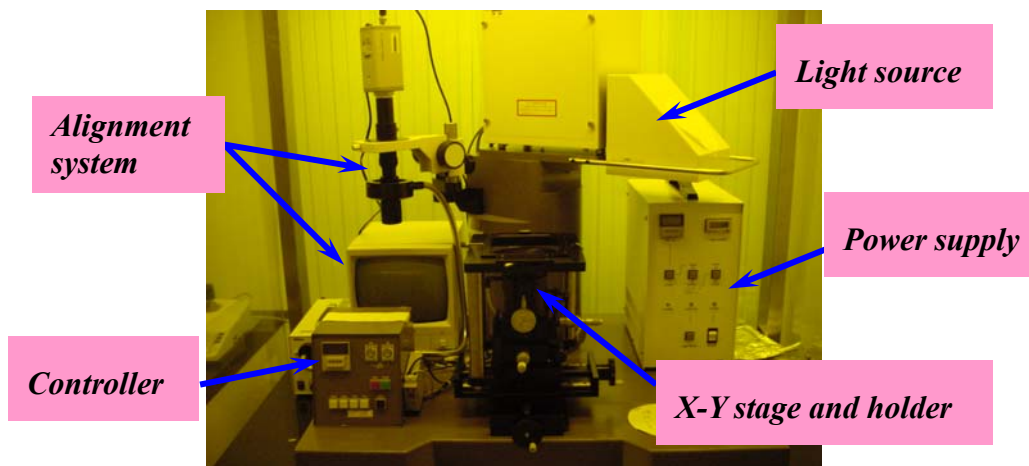


Fig.3-19 The illustration of exposer equipment

3.5 Process of Microcoil/Pad Fabrication

The microcoil supplies a magnetic field about 200~300Oe to magnetize the heated spot on media surface for reading and writing data. A current density is inputted into the microcoil by contact pad. In this process, microcoil and contact pad are made by thick film process and electroplating technology (UV LIGA technology). The process flowcharts are shown in Fig.3-2, and the detail fabrication processes are described in 3-1 section.

The photoresister AZ-4620 8 μ m is defined with mask #4 as shown in

Fig.3-20(a). Then, the Cu metal is deposited by sputtering as the seed layer for electroplating microcoil and contact pad. After lift-off process, the pattern of Cu seed can be achieved as shown in Fig.3-20(b). Due to the microcoil and contact pad are fabricated by UV LIGA technology, so an electroplating mold must be needed. The PR AZ-4620 20 μ m is patterned with mask #5 as the electroplating mold. Then, the Ni microcoil and pad are made by electroplating technique. After removing PR mold, the Ni microcoil and pad will be formed. The fabrication results of electroplating mold and Ni microcoil/contact pad after electroplating process are shown in Fig.3-21(a) and Fig.3-21(b), respectively.

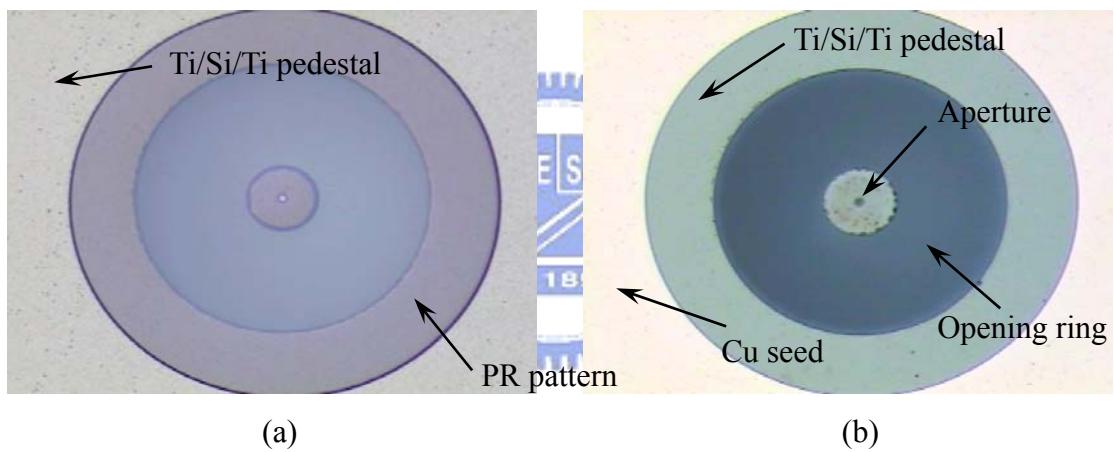


Fig.3-20 (a) The PR pattern for Cu seed lift-off (b) The Cu seed pattern after lift-off

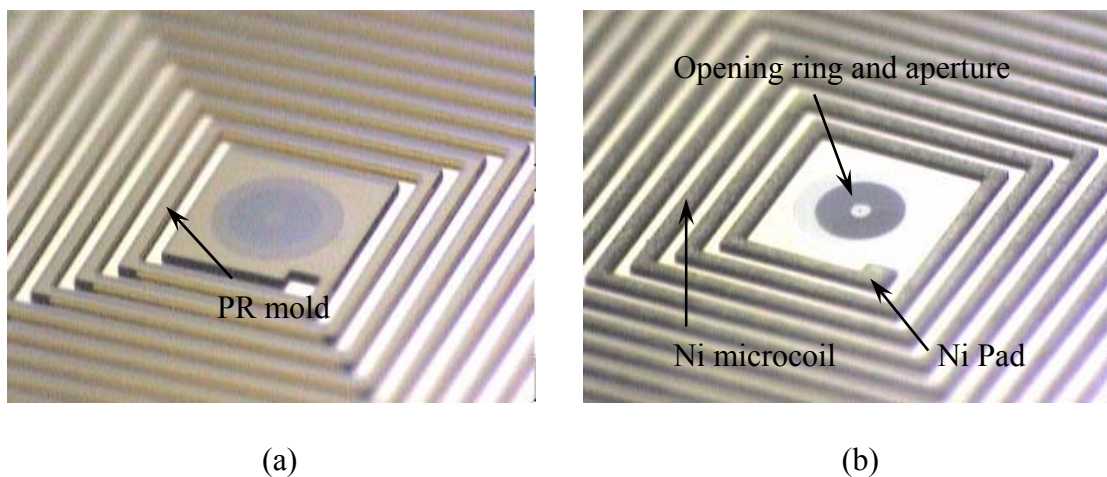


Fig.3-21 (a) The PR mold for electroplating (a) Ni microcoil/pad after electroplating

The width and thickness of microcoil are designed with $50\ \mu\text{m}$ and $15\ \mu\text{m}$, respectively. Furthermore, this planar microcoil has twelve loops, and the contact pad area is $100 \times 100\ \mu\text{m}$ square. The parameters of photolithography are listed in Tab.3-4 and Tab.3-6, respectively. The parameters of electroplating process and basic electroplating theories are listed in Tab.3-7 and Tab.3-8 respectively. Illustration of the electroplating equipment is shown in Fig.3-22.

Tab.3-7 Parameters of electroplating process

Compositions of electroplating solution	Quantity
Ni $(\text{SO}_3\text{NH}_2)_2 \cdot 4\text{H}_2\text{O}$	380gm/L
NiCl ₂	5gm/L
Boron acid	50gm/L
EPC-30	10c.c./L
NPA	2c.c./L
Operation Item	Condition
pH	3.9 ~ 4.2
Temperature	50°C
Maximum current density	14 mA/cm ²
Plating time	35 mins

Tab.3-8 Basic electroplating theories

Nickel Electroplating		
Items	Value	Remarks
Chemical formula	$\text{Ni}^{2+} + 2\text{e}^- \rightarrow \text{Ni}$	
Current density (mA/cm²)	AD	AD : current density
Total charge (Coulomb)	$Q = AD \times 10^{-3} \times A \times t$	A : electroplating area(cm ²) t : electroplating time(mins)
Electric quantity per electron (Coulomb)	$1.6 \times 10^{-9} \text{ C}$	
Molar number	$Q / (1.6 \times 10^{-9})(6.02 \times 10^{23})$	
Volume of Ni production	$\frac{\text{Ni molecular weight}}{2 \times (\text{Density of Ni})}$	Ni molecular weight = 58.71 Specific weight of N = 8.9
Electroplating rate (μm/hr)	$\frac{\text{Volume (Ni)}}{A \cdot t}$	Plating thickness per hour

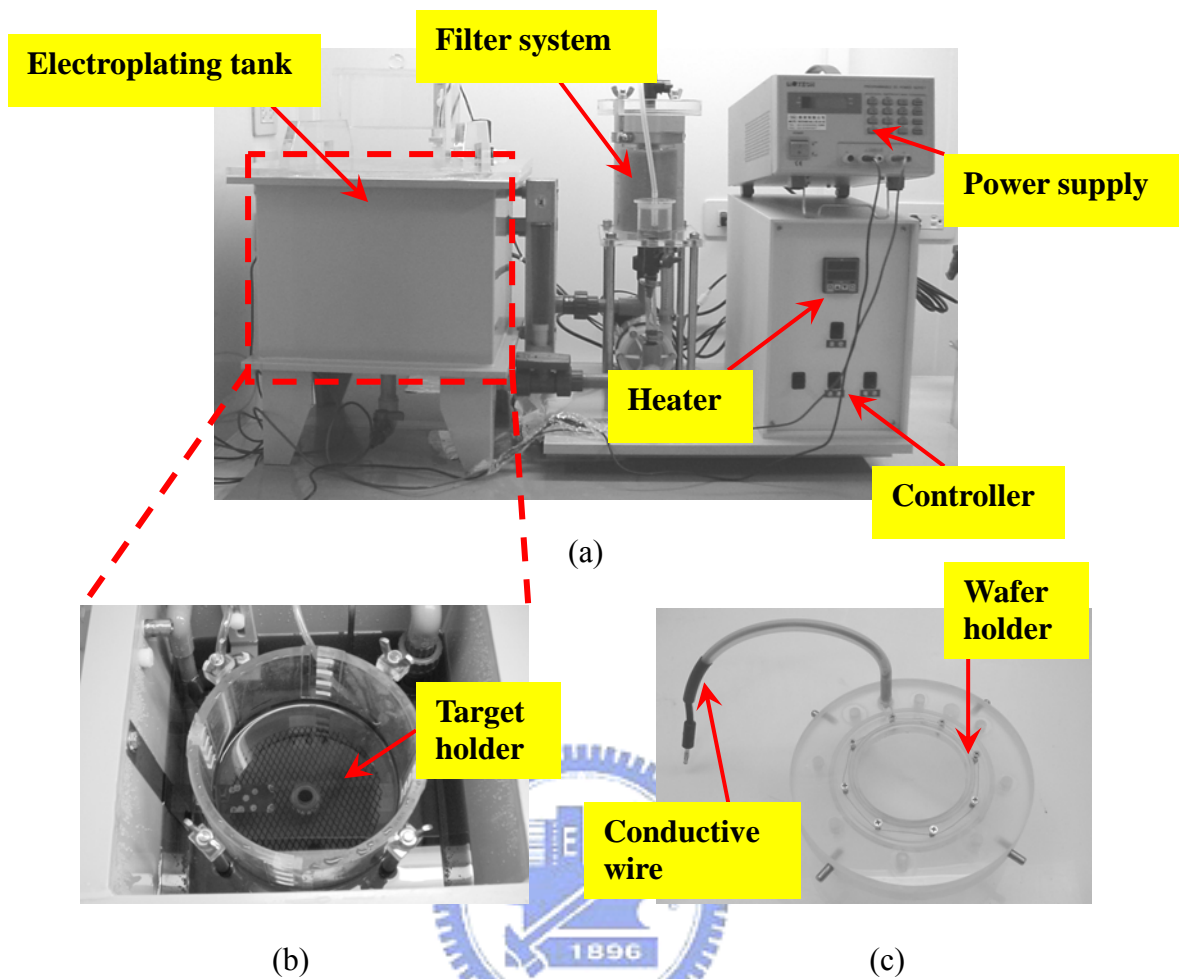


Fig.3-22 (a) Illustration of the electroplating equipment (b) The structure of solution tank (c) Wafer holder and conductive wire

3.6 Integration Structure of NFR Pick-up Head

The integrating structure of NFR pick-up head combining the aperture, SIL and microcoil/pad component together are fabricated by surface micromachining. The aperture and Ni microcoil/pad in NFR pick-up head are fabricated by lift-off and electroplating process, respectively, and the fabrication result is shown in Fig.3-23(a). Figure 3-23(b) shows an aperture in NFR pick-up head. Then, the backside exposure method is adopted to expose the PR AZ-4620 for fabricating SIL component,

as shown in Fig.3-24(a). By self-alignment technique, the SIL and aperture will be alignment together precisely. Finally, the columnar pattern of PR AZ-4620 is heated at 150°C for 2.5 hours by oven. By thermal reflowing process, the SIL can be achieved in NFR pick-up head, as shown in Fig.3-24(b). By using the presented fabrication process in our research, a complete integrating structure of NFR pick-up head will be formed.

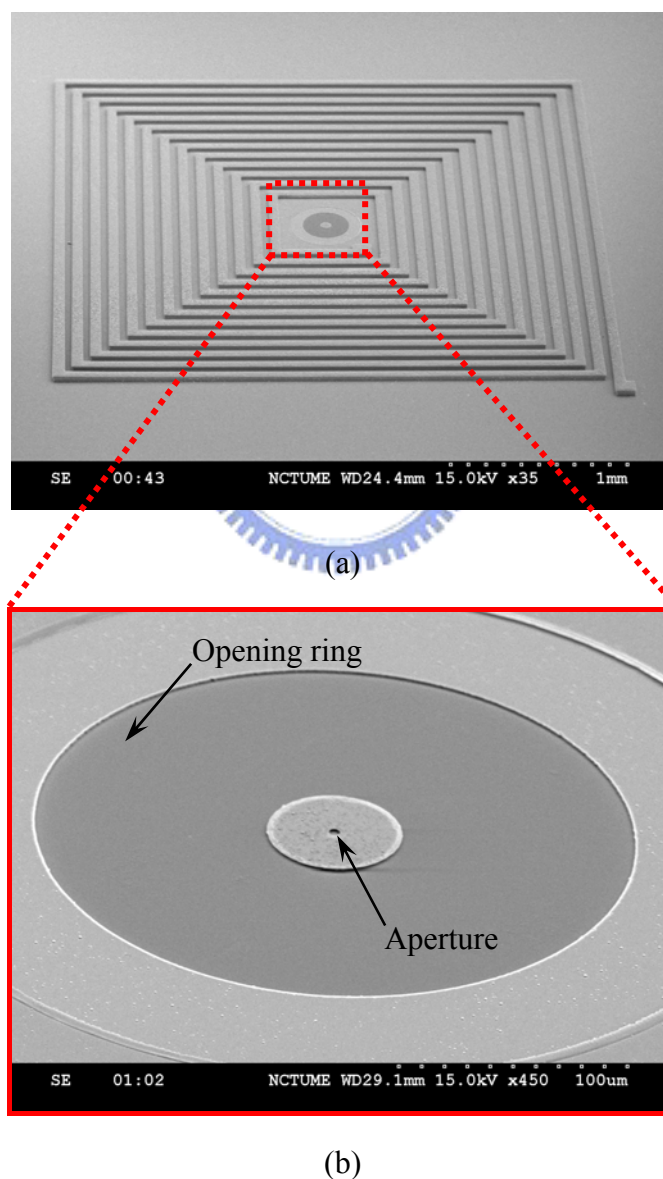
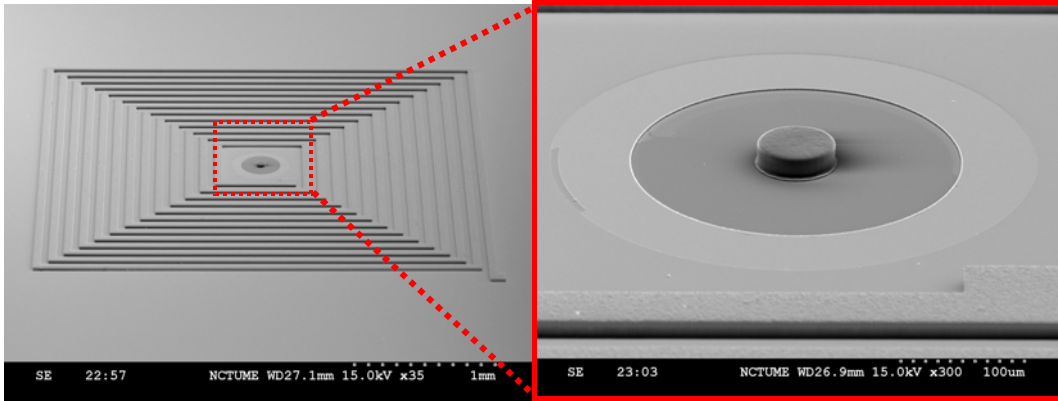
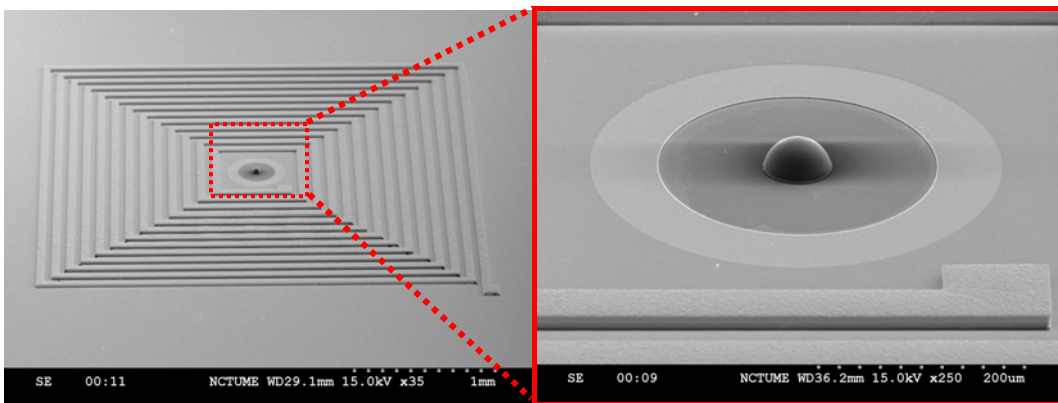


Fig.3-23 (a) Fabrication results of aperture and microcoil/pad (b) an aperture in NFR pick-up head



(a)



(b)

Fig.3-24 The fabrication results of (a) backside exposure step (b) thermal reflow